PROCEEDINGS OF SCIENCE

Studies of rare top quark processes: tZq, $t\gamma q$, $t\bar{t}t\bar{t}$ and flavour changing neutral currents

María Moreno Llácer[*†]
CERN and IFIC (U. Valencia - CSIC)
E-mail: mamolla@cern.ch

The top quark is the heaviest elementary particle and unique among the known quarks since it decays before forming hadronic bound states. Measurements involving top quarks in their final states provide precision tests of the Standard Model and are also sensitive to new physics at the high-energy frontier. The latest cross-section measurements of rare processes with top quarks (tZq, $t\gamma q$ and $t\bar{t}t\bar{t}$ production) as well as searches for flavour changing neutral currents are presented here using 13 TeV proton-proton collisions recorded by the ATLAS and CMS detectors at the Large Hadron Collider at CERN. The measured values are compared to the most accurate theoretical calculations. All these measurements probe the top quark couplings.

7th Annual Conference on Large Hadron Collider Physics - LHCP2019
20-25 May, 2019
Puebla, Mexico

[*]Speaker.
[†]on behalf of the ATLAS and CMS Collaborations

PoS(LHCP2019)106

1. Introduction

Precise measurements of the couplings of the top quark, the heaviest known elementary particle, are an important check of the internal consistency of the Standard Model (SM) of particle physics and could provide hints of possible new physics beyond the SM (BSM). The large amount of proton-proton collision data at the CERN Large Hadron Collider (LHC) allows for experimental reach of rare processes with top quarks in their final state. Rare production mechanisms, such as tZq, $t\gamma q$ and $t\bar{t}t\bar{t}$, are now accessible with the LHC Run 2 dataset. These processes are particularly interesting since they provide direct access to the neutral top quark couplings and are also sensitive to new physics effects and effective field theories (EFT). In addition, processes producing a single-top quark, like the associated production of tZq and $t\gamma q$, can give very valuable information since the top quark is produced via electroweak interaction and thus polarised; while $t\bar{t}t\bar{t}$ process can be used to constrain the magnitude and CP properties of the top quark Yukawa coupling to the Higgs boson. In the SM, the top quark decays almost exclusively to W boson and b quark. Decays of the top quark to a neutral gauge or Higgs boson and a up or charm quark through the so-called flavour-changing neutral current (FCNC) are highly suppressed in the SM due to the Glashow-Iliopoulos-Maiani mechanism with branching ratios around 10^{-14}. However, new physics models like the quark-singlet (QS) model or the two-Higgs-boson-doublet model with flavour violating Yukawa couplings (2HDM-FV) bring them up to 10^{-4}.

In this contribution, the latest results on rare processes with top quarks from the ATLAS [1] and CMS [2] collaborations are discussed. They include first experimental cross-section measurements for tZq, $t\gamma q$ and $t\bar{t}t\bar{t}$ production and limits on the rates of FCNC processes in the production or decay of the top quark. The measured values are compared to the most accurate theoretical calculations. Most of the analyses discussed here used only a fraction of the LHC 13 TeV dataset and are being updated at the time of writing.

2. Observation of tZq process and its cross-section measurement

The tZq process in particular is an interesting process since it is sensitive to the top-Z and WWZ couplings. In addition, it is a background for many searches such as the production of tZ through FCNC processes. Representative Feynman diagrams for tZq and $tllq$ production in proton-proton collision are shown in Figure 1. The Z boson can arise from initial- or final-state radiation and via triple gauge couplings.

The measurements of the inclusive tZq production cross-section were performed using the trilepton channel. It is the most promising one despite the small branching ratio. Events with exactly three leptons, electrons and/or muons, well-isolated and with different transverse momentum (p_{T}) cuts are used to maximise the signal-to-background ratio (S/B). The Z boson is reconstructed from a pair of leptons with opposite-sign and same-flavour (OSSF). The OSSF pair is required to have an invariant mass within a window around the Z boson mass. The remaining lepton is associated to the W boson that is assumed to come from the top quark decay. In addition, many quality cuts are applied to increase the S/B.

CMS [3] requires events with at least two jets being at least one of them b-tagged which is used to reconstruct the top quark. The remaining jet with the highest p_{T} in the event, typically

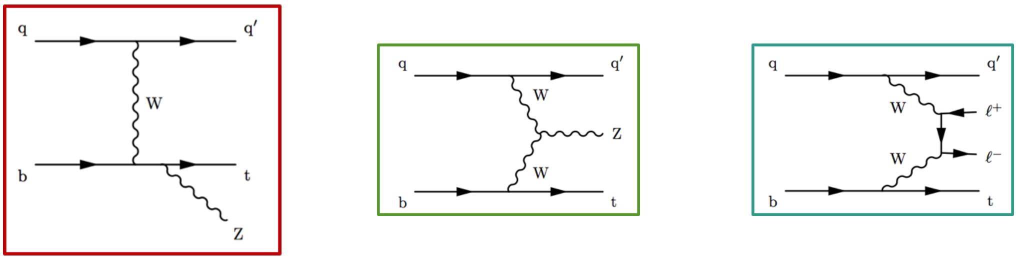

Figure 1: Example Feynman diagrams of the lowest-order amplitudes for the tZq process. The Z boson can be radiated from an initial- or final-state quark (the latter via the top-Z coupling as shown in the left diagram), or coupled to the W boson via triple gauge couplings (WWZ coupling) or offshell ll production (middle and right diagrams). In the four-flavour scheme, the bottom quark (b) originates from gluon splitting.

found in the forward region of the detector, is labeled the "recoiling jet". Events are divided based on the number of jets into three categories, collectively referred to as signal regions (SRs): "SR-2/3j-1b", "SR-4j-1b" and "SR-2b". In each of them, a boosted decision tree (BDT) is employed to combine many input variables to enhance the S/B. The kinematic properties of the recoiling jet (p_{T} and pseudo-rapidity η) are the most effective variables in separating tZq signal and background events. Figure 2 shows the BDT distribution for the most sensitive SR and the Z boson p_{T} in events with a BDT discriminant value greater than 0.5. Furthermore, two control regions (CRs) are defined for the dominant backgrounds which is diboson production. The tZq cross-section is extracted using a binned maximum likelihood fit that is performed on the full BDT distributions in the three SRs and the number of jets in the WZ and ZZ CRs. All sources of systematic uncertainties are taken into account as nuisance parameters in the fit. The analysis is performed using data collected in 2016 and 2017, corresponding to an integrated luminosity of 77.4 fb^{-1}. The observed and expected signal significances are well above 5 standard deviations from the background-only hypothesis, and thus the observation of tZq SM process. The tZq cross-section is measured to be $\sigma(pp \to tZq \to tllq)$=111 $\pm$ 13(stat) $^{+11}_{-9}$(syst) fb where l refers to an electron, muon or τ lepton, for invariant masses of the dilepton pair larger than 30 GeV. The theoretical cross-section in the same fiducial volume is of 94.2 $\pm$ 3.1 fb, which is computed at next-to-leading-order in perturbative QCD using the NNPDF3.0 PDF set in the five-flavour scheme. The systematic uncertainties with the largest contribution to the final measurement are those associated with the non-prompt lepton background prediction, the lepton selection efficiency, the modelling of final-state radiation and the jet energy scale.

ATLAS [4] performed a similar measurement using only events with exactly two jets, being exactly one b-tagged plus one untagged (light-flavour) jet that tends to be in the forward direction. The dataset used has an integrated luminosity of 36.1 fb^{-1}, recorded in 2016. The major backgrounds are diboson, $t\bar{t}$ and Z+jets production. The analysis also uses a multivariate analysis technique, in this case a neural network (NN) with ten input variables. Among them, the p_{T} and η of the untagged jet and mass of the reconstructed top quark are the ones with higher separation power. The observed signal significance is 4.2 standard deviations, compared to 5.4 expected.

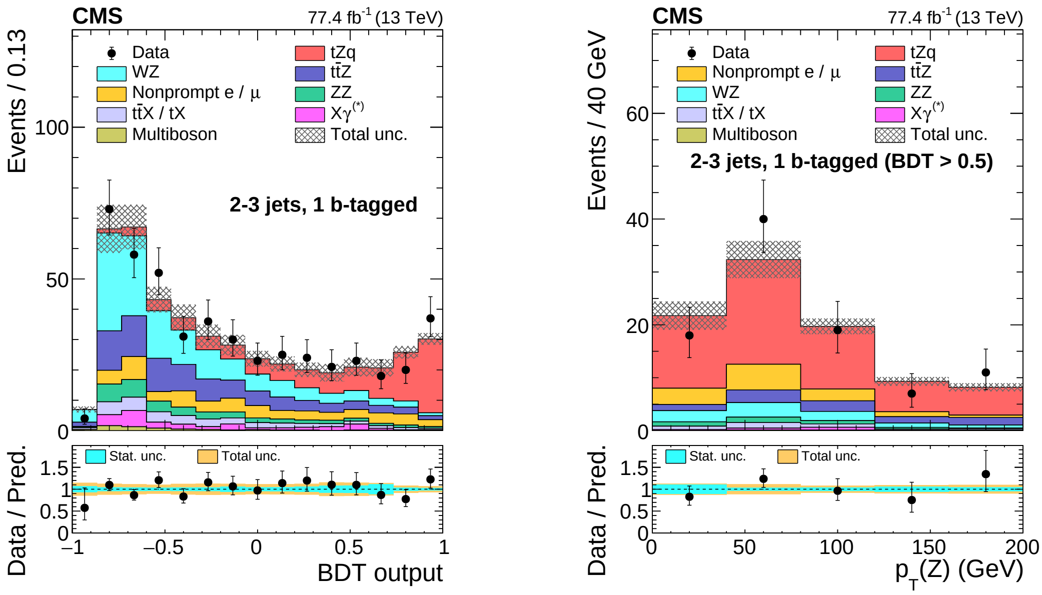

Figure 2: BDT distribution for events in the tZq SR-2/3j-1b (left) and the Z boson transverse momentum for events with high BDT score in the same region (right) [3]. Observed data (points) are compared with postfit expected predictions (shaded histograms). The vertical bars on the points represent the statistical uncertainties in the data. The hatched regions show the total uncertainties in the background. The lower panels display the ratio of the observed data to the predictions, including the tZq signal, with inner and outer shaded bands representing the statistical and total uncertainties, respectively, in the predictions.

3. First evidence of the SM $t\gamma q$ production

In the single-top quark production in association with a photon ($t\gamma q$), photons can arise either from initial- or final-state radiation and via triple gauge couplings. The signature is sensitive to anomalous gauge $WW\gamma$ couplings and possible top$\rightarrow$ γq FCNC. The first evidence of events consistent with $t\gamma q$ production has been recently reported by CMS collaboration [5]. The analysis is based on the 2016 dataset which corresponds to an integrated luminosity of 35.9 fb^{-1}. Events are selected with exactly one high-p_{T} well-isolated muon, while events with electrons are not included in the analysis because of the high background. In addition, they are required to have one isolated photon (p_T>25 GeV and $|\eta|$ <1.44), an imbalance in transverse momentum from an undetected neutrino (ν) and at least two jets, of which exactly one is identified as associated with the hadronization of a b-quark. In order to select well-isolated objects, the photon is required to be separated from the b-jet, the light-flavour jet, and any muon candidate by ΔR(γ,X)>0.5, where X stands for μ, b-jet or light-flavour jet. After this SR selection, the total number of observed events is 2535 of which 2401 $\pm$ 178 events are expected from the SM background in absence of $t\gamma q$ signal. The expected number of signal events from the SM is 154 $\pm$ 24. The dominant background is $t\bar{t}$+γ which amounts to 55% of the total background yield. The next background contribution arises from a misidentified jet, such as $t\bar{t}$, W+jets, Z+jets process. The misidentified photon background is estimated from the measurement of the p_{T}-dependent probability for a jet to be reconstructed as a photon using events with looser identification criteria for photons. A multivariate discriminant based on eight topological and kinematic event properties is employed to separate signal from background processes. The pseudo-rapidity of the light-flavour jet and cos θ, which is the cosine of the angle between the muon candidate and the light-flavour jet in the top quark rest-frame, are the two most discriminant variables. Figure 3 shows the BDT distribution and the most discriminant variable for data, signal and all the backgrounds. The templates for signal, $t\bar{t}$+γ, $W\gamma$+jets, $Z\gamma$+jets, the misidentified photon background and the sum of all other backgrounds are taken from simulation except for $t\bar{t}$+γ and misidentified photons. The latter is obtained with the method described above, calculating the yield as a function of BDT output. The template for $t\bar{t}$+γ is estimated from data using a CR defined by requiring exactly two b-tagged jets, while keeping all other selection criteria the same as for the SR. The requirement of two b-tagged jets ensures a high contribution from $t\bar{t}$+γ, while suppressing the contributions from all other processes. In addition, $W\gamma$+jets is validated in data in a validation region defined substituting of the signal b-jet requirement by a b-jet veto. In order to extract the signal cross-section and $t\bar{t}$+γ background normalization, a simultaneous binned likelihood fit is performed on the BDT distribution in the SR and the $t\bar{t}$+γ CR. The observed significance is 4.4σ while the predicted significance is 3σ. Furthermore, the fiducial cross-section for isolated photons with transverse momentum greater than 25 GeV in the central region of the detector is extracted. The measured product of the cross-section and branching ratio is $\sigma(pp \to t\gamma q)BR(t \to \mu\nu b) = 115 \pm 17(\text{stat}) \pm 30(\text{syst})$ fb, which is consistent with the Standard Model prediction within this fiducial phase space of 81 $\pm$4 fb.

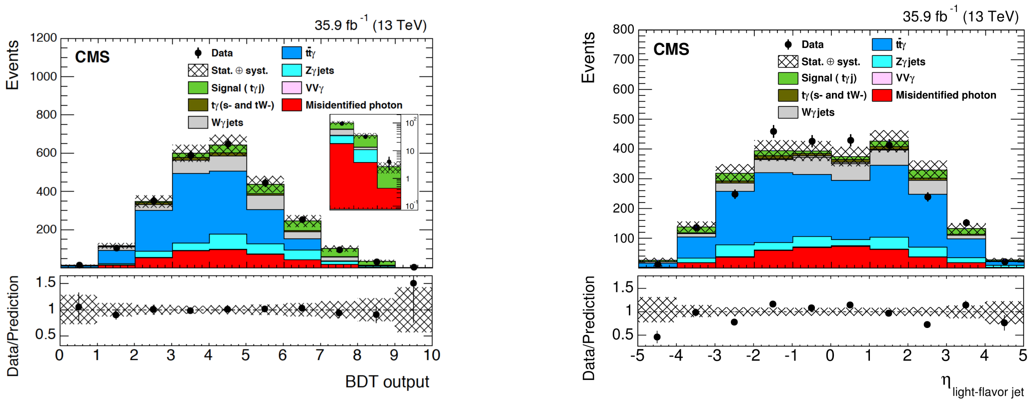

Figure 3: The BDT output (left) and pseudo-rapidity of the light-flavour jet (right) distributions for data and SM predictions after performing the fit [5]. The inset presents a closeup of the last three bins plotted on log scale. The hatched band shows the statistical and systematic uncertainties in the estimated $t\gamma q$ signal and background yields, and the vertical bars on the points represent the statistical uncertainties of the data. The ratio of the data to the SM prediction is shown in the bottom panel.

4. Very close to find evidence of $t\bar{t}t\bar{t}$ production

The production of four top quarks, $t\bar{t}t\bar{t}$, is one of the most spectacular mechanisms at the LHC. It is quite energetic since it requires almost 700 GeV. This process has not been observed yet, but has vast sensitivity to new physics and also offers an alternative way to access the top quark Yukawa coupling (the largest coupling of the Higgs boson). The $t\bar{t}t\bar{t}$ process has a very busy signature, since there are many jets in the final state, being four of them originated from b-quarks.

The experimental analyses are split into different channels depending on the decay of the W boson (either hadronically or leptonically) from each top quark and combined afterwards. Broadly the separation is: i) one or two opposite-sign charged leptons ("1L+2LOS") and ii) two same-sign or three charged leptons ("2LSS+3L"). Again, charged leptons are only referring to electrons or muons. The "1L+2LOS" channels have large statistics due to the large (>50%) branching ratio, although also overwhelming backgrounds. Contrary, "2LSS+3L" channels are quite pure but account only for 12% branching ratio. Both ATLAS and CMS collaborations have recently reported results for the two analyses. All of them analysed around 36 fb^{-1} of data except CMS results for "2LSS+3L" for which the whole LHC Run 2 was used.

4.1 1L and 2LOS channels

Data events in the single-lepton and opposite-sign dilepton channels are characterized by the presence of one or two isolated electrons or muons with high transverse momentum and multiple jets. In the case of ATLAS [6], events with at least five (four) jets and being at least two b-tagged are preselected in the "1L" ("2LOS") channels. Afterwards, they are categorised according to the multiplicities of jets (j), b-jets (b) and mass-tagged reclustered large-R jets (J), referred to as "mj, nb, pJ". As displayed in Figure 4, a total of twenty signal regions are considered.

Both channels are dominated by the $t\bar{t}$+jets background, mainly $t\bar{t}b\bar{b}$, which is not well known theoretically. Therefore, a data-driven approach called "tag rate function for $t\bar{t}$ events (TRF$_{t\bar{t}}$)" is used for its estimation. The method assumes that the probability of b-tagging an additional jet is independent of the number of additional jets. With this assumption, the tagging probability, as a function of kinematic properties of the jet, can be estimated in lower jet multiplicity events and then applied to data events with same jet multiplicity as in SR events but lower b-tagged jet multiplicity (see Figure 4). For the "1L" channel, the background from events with a fake or non-prompt lepton is estimated directly from data using the matrix method. In the "2LOS" channel, this background is estimated from Monte Carlo simulation. A simultaneous fit to the H_T^{had} (the scalar sum of the transverse momenta of all the selected jets in the event) distribution in each of the twenty SRs (see some of them in Figure 5) is performed and results in an observed (expected) 95% confidence level (CL) upper limit on $t\bar{t}t\bar{t}$ production cross-section of 47 fb (33 fb). Consequently, the upper limit on $\sigma(t\bar{t}t\bar{t})$ is measured to be 5.1 (3.6) times the SM prediction. This result is included in the summary plot on the right of Figure 7.

The production of four top quarks is a unique signature that provides information about models that predict enhanced interactions of the third generation quarks. Thus, the experimental results are interpreted in the EFT framework and yield limits on dimension-6 four-fermion operators coupling to third generation quarks. Such interpretation gives an observed (expected) upper limit of 21 fb (22 fb) at 95% CL. In this case, the SM four top quark production is considered as a background. This result is lower than the limit for the SM $t\bar{t}t\bar{t}$ production as the contact interaction tends to result in final state objects with larger momenta.

In the case of CMS [7], events are categorised based on the number of jets, b-jets and lepton flavour. Later, BDTs are used with two roles: to identify the top quarks and to improve the discrimination between signal and background. The BDT for identifying hadronically decaying top quarks ($t \to Wb \to jjb$) classifies combinations of three jets (trijet) on how consistent they are with the trijet originating from the all-hadronic decay of a top quark, rather than from other sources such

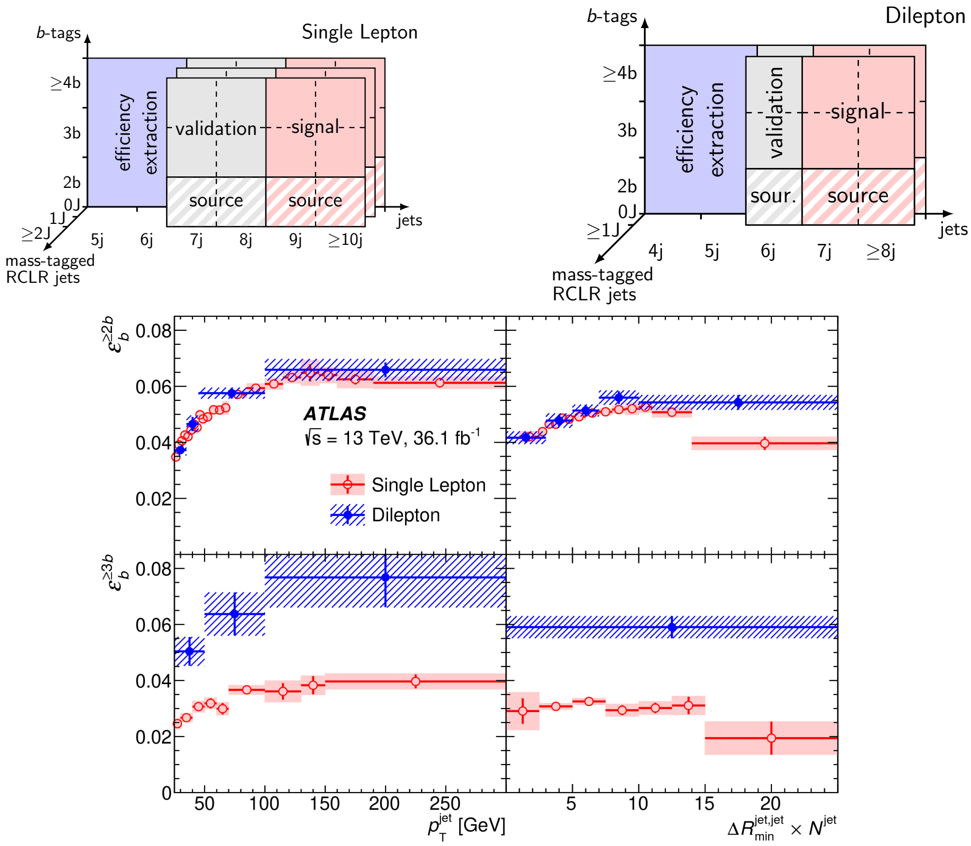

Figure 4: Schematic view of the different analysis regions in the single-lepton (top left) and dilepton (top right) channels. The three axes represent the jet multiplicity, the b-tagged jet multiplicity and the mass-tagged reclustered large-R jet multiplicity. The efficiency extraction region in each channel is defined inclusively in the mass-tagged reclustered large-R jet multiplicity. The bottom figure shows the values of the per-jet b-tagging probability for $t\bar{t}$+jets events, separately for single-lepton and dilepton channels, as a function of some jet properties for data events with at least two or three b-jets. Source: [6]

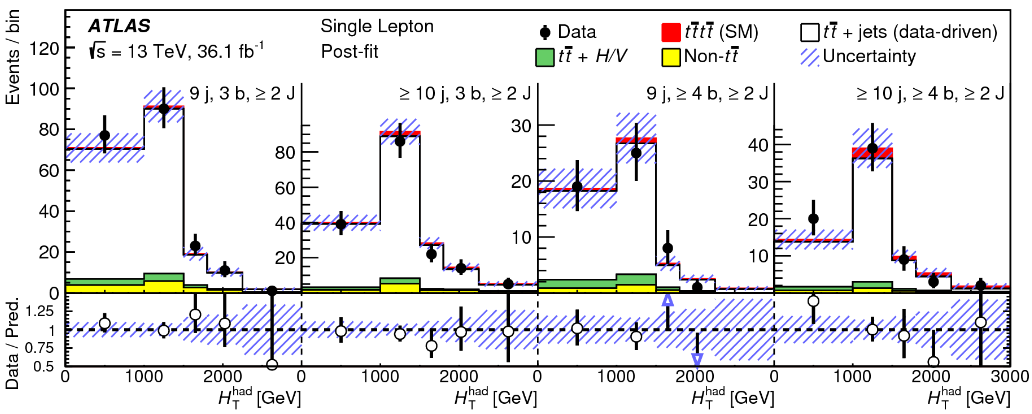

Figure 5: Comparison between data and prediction of the H_T^{had} distributions in some of the single-lepton signal regions after the combined fit to data in both the single-lepton and dilepton channels [6].

as initial- or final-state radiation. For the second BDT, global event and jet properties are used to discriminate $t\bar{t}t\bar{t}$ from $t\bar{t}$ production. In this analysis, $t\bar{t}$+jets events are modelled using Monte Carlo simulations, in particular Powheg+Pythia8 with the top quark p_{T} reweighted to recent calculations. The dominant uncertainties are limited by data statistics, b-tagging and modelling of $t\bar{t}$ events. No statistically significant deviation from the SM background prediction is observed, and upper limits to the cross-section are calculated and are shown in the summary plot of Figure 7. As in the case of ATLAS results, 95% CL intervals for selected four-fermion EFT operators are reported.

4.2 2LSS and 3L channels

These channels are dominated by lepton fakes and $t\bar{t}V$ ($V = W, Z$) backgrounds. Data-driven techniques are used for fake and non-prompt lepton backgrounds, which are estimated with the matrix method or "tight-to-loose" method, and charge misidentification in the "2LSS" channel. Irreducible $t\bar{t}V$ backgrounds are modelled by Monte Carlo simulations.

In the case of ATLAS [8], 36 fb^{-1} of data are used and the strategy followed is a cut-based analysis with eight signal regions and six validation regions. The SM $\sigma(t\bar{t}t\bar{t})$ upper limit obtained is 69 fb (29 fb) for the observed (expected).

The CMS result [9] uses the full LHC Run 2 dataset (136 fb^{-1}) and two strategies are followed to enhance signal sensitivity: first a cut-based simple classification based on lepton and jet multiplicity and jet flavour, and second a BDT taking advantage of kinematic variables related to leptons and jets. The main backgrounds with prompt leptons, $t\bar{t}W$ and $t\bar{t}Z$, are modelled by simulations but their normalisation is constraint using dedicated CRs. In addition, the number of additional jets is corrected based on initial- and final-state jet multiplicity measurements in dilepton $t\bar{t}$ events. These correction factors range from 1.46 to 0.77. The flavour of additional jets (in this case also for $t\bar{t}H$) is corrected based on $t\bar{t}b\bar{b}/t\bar{t}j\bar{j}$ measurement (R = 1.7 $\pm$ 0.6) [10]. This correction results in a 70% increase of events produced in association with a pair of additional b-jets. Figure 6 shows the jet multiplicity for all the cut-based SRs and for the $t\bar{t}W$ CR. The two approaches find consistent results compatible with next-to-leading-order SM predictions. The observed (expected) significance of the BDT analysis is 2.6 (2.7) standard deviations, and the $\sigma(t\bar{t}t\bar{t})$ is measured to be $12.6^{+5.8}_{-5.2}$ fb. The obtained BDT distribution and a summary with all the upper limits are shown in Figure 7. These results are used to constrain the Yukawa coupling of the top quark, yielding a 95% confidence level limit of $|y_t/y_t^{SM}| < 1.7$. Limits are also set on the production of a heavy scalar and a pseudoscalar in a type II 2HDM scenario, with exclusions in the mass ranges of 350-470 GeV and 350-550 GeV, respectively.

5. Searches for rare top quark decays: flavour changing neutral currents

Searches for FCNC interactions have been performed both in the decay of one of the top quarks from $t\bar{t}$ production and also in single-top quark production. In the case of $t\bar{t}$ events, one top quark decays through the $t \rightarrow Xq$ ($X = H, g, Z, \gamma$; $q = u, c$) FCNC channel, and the other through the SM dominant mode $t \rightarrow Wb$. The following subsections review the latest results on these FCNC searches carried out by the ATLAS and CMS experiments. These have used only a fraction (2015 and 2016 datasets) of the LHC Run 2 data collected at 13 TeV.

PoS(LHCP2019)106

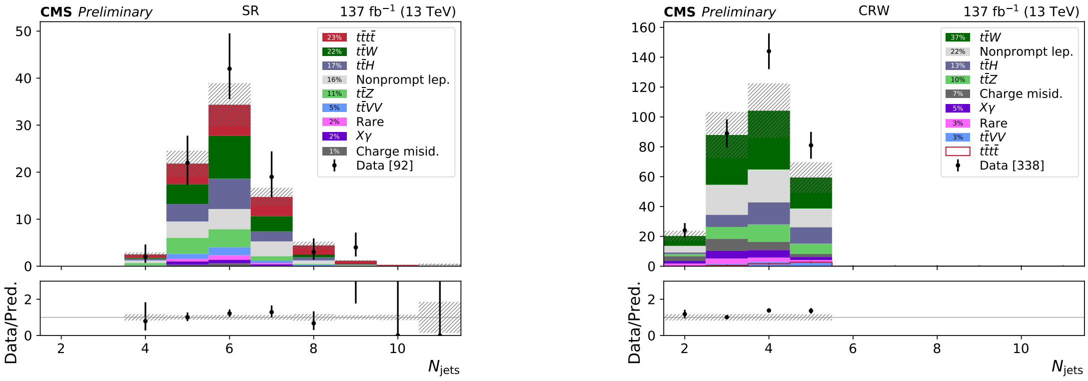

Figure 6: Jet multiplicity for all the cut-based $t\bar{t}t\bar{t}$ SRs and $t\bar{t}W$ CR defined in the "2lSS+3L" CMS analysis, before fitting to data, where the last bins include the overflows [9]. The hatched areas represent the total uncertainties in the SM signal and background predictions. The $t\bar{t}t\bar{t}$ signal assumes the SM cross-section prediction. The lower panels show the ratios of the observed event yield to the total prediction.

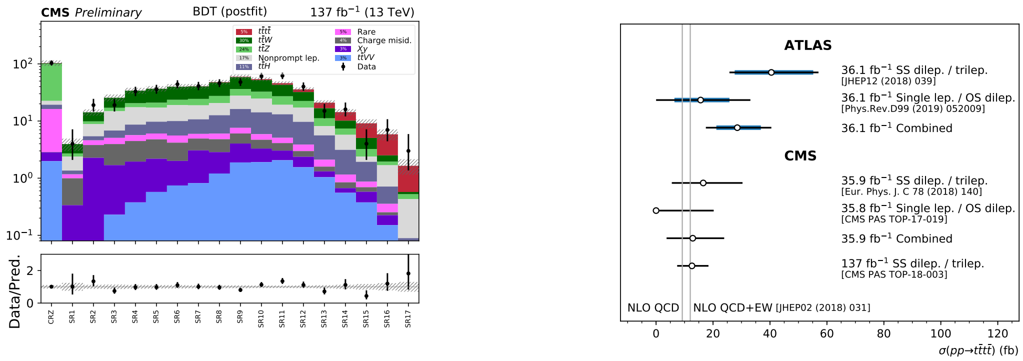

Figure 7: Left: Observed yields in the BDT-based analysis compared to the post-fit predictions for signal and background processes for the "2lSS+3L" CMS analysis [9]. Right: Summary plot with the $\sigma(t\bar{t}t\bar{t})$ upper limits for the "1L+2LOS" and "2LSS+3L" results from ATLAS and CMS.

5.1 Final states with a Z boson

In the search for $t\to Zq$ decays, both ATLAS [11] and CMS [12] focus on the same final state, by selecting events with exactly three leptons (electrons and/or muons), comprising a pair of two OSSF leptons required to have an invariant mass within 10 GeV of the Z boson mass and at least two jets, where one (ATLAS) or more (CMS) is b-tagged. This so-called "decay mode" signature results from $t\bar{t}$ production followed by a $t\to Zq$ interaction. CMS also considers the "production mode", where a single incoming parton decays as $q\to Zt$. There, the jet requirements are lowered to exactly one jet, which must also be b-tagged. The main backgrounds, diboson production, non-prompt leptons (fakes) and rare processes with top quarks (tZq, $t\bar{t}Z$), are estimated in a number of dedicated CRs. Multivariate analysis approaches are used to separate signal from background. The complete statistical analysis yields limits for the branching ratio BR($t\to Zu$)$<1.7\times10^{-4}$(2.4×10^{-4}) and BR($t\to Zc$)$<2.4\times10^{-4}$(4.5×10^{-4}) for ATLAS (CMS). The left plot of Figure 8 shows the discriminating variable distribution after the fit for all different CMS leptonic channels in "decay mode" for tZu signal. The dominant uncertainties come from the modelling and normalisation of the background processes.

5.2 Final states with a Higgs boson

Several channels are defined depending on the decay mode of the Higgs boson. CMS targets the final state $H \to b\bar{b}$ [13] by selecting events with exactly one lepton and at least three jets, two or more of which must be b-tagged. These are further split according to (b-)jet multiplicity into five orthogonal SRs, and two BDTs are trained to further enhance the signal sensitivity. The first one uses the likelihood event reconstruction and b-jet assignments to discriminate between three event hypotheses: $t\bar{t}$-like and single-top-like signals, and semileptonic $t\bar{t}$ background, where one of the top quarks decays semileptonically and the other one hadronically. A number of b-jet related kinematic and tagging variables are then used to train the second BDT, aiming in differentiating between the signal events that are generated either for κ_{Hut} or κ_{Hct} coupling against the sum of all backgrounds. The limits at the 95% CL obtained in the $t \to Hu$ and $t \to Hc$ branching fractions are very similar, at around 4.7×10^{-3}.

ATLAS similarly employs a multivariate approach in the multi-lepton final state [14], targeting the $H \to WW^*$ decay in same-sign dilepton and trilepton selections, using two BDTs to reject background and increase the sensitivity (specifically to κ_{Hut}). The diphoton final state explored in Ref. [15] targets the $H \to \gamma\gamma$ decay, constructing SRs in the all-hadronic or leptonic final states. Higgs bosons are enriched in the sample by requiring 100<$m_{\gamma\gamma}$<160 GeV, but this particular channel is still largely dominated by statistical uncertainties. The $H \to b\bar{b}$ mode [16], on the other hand, is the only tHq analysis to evade this limitation on data statistics. Thanks to the large number of SRs which have different background composition, these processes are more efficiently constrained. A companion search in the $H \to \tau^+\tau^-$ channel is presented in Ref. [16], using BDTs trained on the masses and kinematics of the reconstructed final state objects, divided into four signal regions according to jet multiplicity and decay of the τ leptons. ATLAS also performs a combination of all these searches at 13 TeV, yielding observed 95% CL upper limits on the $t \to Hu$ and $t \to Hc$ branching ratios of 1.2×10^{-3} and 1.1×10^{-3}, respectively (see right plot of Figure 8).

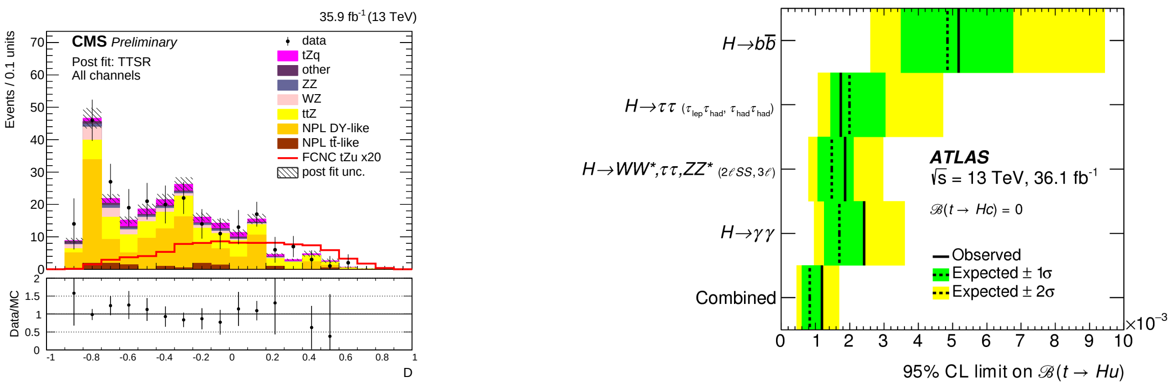

Figure 8: Left: The discriminating variable distribution after the fit for all different leptonic channels in "decay mode" for the CMS FCNC tZu search [12]. Right: Upper limits for all the channels defined in the ATLAS $t \to Hc$ FCNC search [16].

5.3 Summary of the current limits for FCNC searches

Data are compatible with the background-only hypothesis in all the channels explored, therefore upper limits on branching ratios are set at 95% confidence level using the CLs method. The values obtained from ATLAS and CMS results are summarised in Figure 9, tantalisingly close to certain BSM predictions.

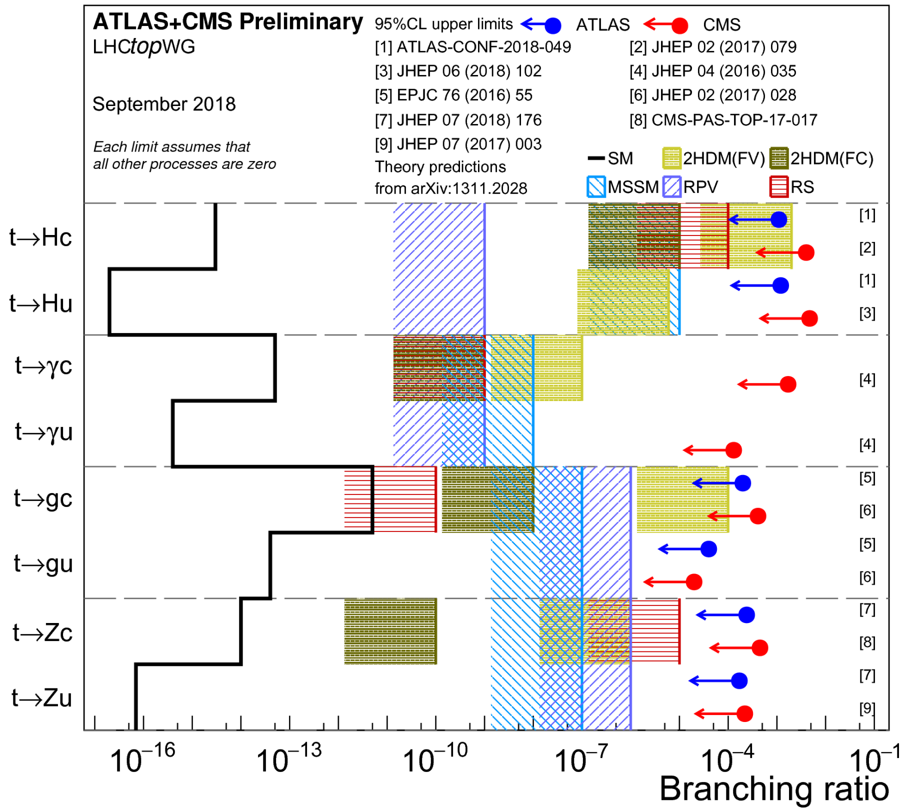

Figure 9: Summary of the current 95% confidence level observed upper limits on the branching ratios of the top quark decays via flavour changing neutral currents to a quark and a neutral boson $t \to Xq$ ($X = H, g, Z, \gamma$; $q = u, c$) by the ATLAS and CMS Collaborations compared to several new physics models. Source: LHC Top WG [17].

6. Summary

Many new measurements of rare top quark production mechanisms have been performed in the past months by the ATLAS and CMS collaborations with data from the LHC Run 2. In general, good agreement with the SM predictions is observed. The associated production of single-top quarks with neutral electroweak bosons is moving from searches to precision measurements, reaching accuracies of around 15% for tZq and 30% $t\gamma q$. Four top quarks production is approaching SM sensitivity. Competitive limits on the branching ratios of rare FCNC top decays have been obtained, approaching sensitivity to BSM models.

References

[1] ATLAS Collaboration, 2008 JINST 3 S08003.

[2] CMS Collaboration, 2008 JINST 3 S08004.

[3] CMS Collaboration, Phys. Rev. Lett. 122,132003 (2019).

[4] ATLAS Collaboration, Physics Letters B 780 (2018) 557-577.

[5] CMS Collaboration, Phys. Rev. Lett. 121,221802 (2018).

[6] ATLAS Collaboration, Phys. Rev. D 99 (2019) 052009.

[7] CMS Collaboration, CMS-PAS-TOP-17-019, https://cds.cern.ch/record/2666712.

[8] ATLAS Collaboration, JHEP 12 (2018) 039.

[9] CMS Collaboration, CMS-PAS-TOP-18-003, https://cds.cern.ch/record/2668710.

[10] CMS Collaboration, Phys. Lett. B776(2018) 355.

[11] ATLAS Collaboration, JHEP 07 (2018) 176.

[12] CMS Collaboration, CMS-PAS-TOP-17-017, https://cds.cern.ch/record/2292045.

[13] CMS Collaboration, JHEP 06 (2018) 102.

[14] ATLAS Collaboration, Phys. Rev. D 98 (2018) 032002.

[15] ATLAS Collaboration, JHEP 10 (2017) 129.

[16] ATLAS Collaboration, JHEP 05 (2019) 123.

[17] LHC TopWG summary plots:
https://twiki.cern.ch/twiki/bin/view/LHCPhysics/LHCTopWGSummaryPlots.

PoS(LHCP2019)106